JACS
JOURNAL OF THE AMERICAN CHEMICAL SOCIETY

Subscriber access provided by American Chemical Society

Article

Single d-Metal Atoms on F and F Defects of MgO(001): A Theoretical Study across the Periodic Table

Konstantin M. Neyman, Chan Inntam, Alexei V. Matveev, Vladimir A. Nasluzov, and Notker Rsch

J. Am. Chem. Soc., **2005**, 127 (33), 11652-11660• DOI: 10.1021/ja052437i • Publication Date (Web): 30 July 2005

Downloaded from http://pubs.acs.org on March 25, 2009

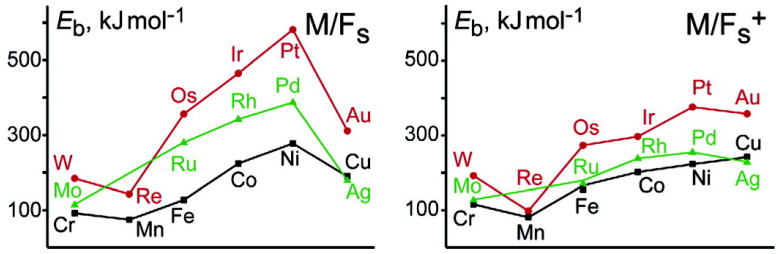

More About This Article

Additional resources and features associated with this article are available within the HTML version:

- Supporting Information
- Links to the 17 articles that cite this article, as of the time of this article download
- Access to high resolution figures
- Links to articles and content related to this article
- Copyright permission to reproduce figures and/or text from this article

View the Full Text HTML

ACS Publications
High quality. High impact.

Journal of the American Chemical Society is published by the American Chemical Society. 1155 Sixteenth Street N.W., Washington, DC 20036

J|A|C|S
ARTICLES
Published on Web 07/30/2005

Single d-Metal Atoms on F_s and F_s^+ Defects of MgO(001): A Theoretical Study across the Periodic Table

Konstantin M. Neyman,*,† Chan Inntam,‡ Alexei V. Matveev,‡
Vladimir A. Nasluzov,§ and Notker Rösch*,‡

Contribution from the Department Chemie, Technische Universität München, 85747 Garching, Germany, Institució Catalana de Recerca i Estudis Avançats (ICREA) and Departament de Química Física i Centre Especial de Recerca en Química Teòrica, Universitat de Barcelona i Parc Científic de Barcelona, 08028 Barcelona, Spain, and Institute of Chemistry and Chemical Technology, Russian Academy of Sciences, 660049 Krasnoyarsk, Russia

Received April 14, 2005; E-mail: konstantin.neyman@icrea.es; roesch@ch.tum.de

Abstract: Single d-metal atoms on oxygen defects F_s and F_s^+ of the MgO(001) surface were studied theoretically. We employed an accurate density functional method combined with cluster models, embedded in an elastic polarizable environment, and we applied two gradient-corrected exchange-correlation functionals. In this way, we quantified how 17 metal atoms from groups 6−11 of the periodic table (Cu, Ag, Au; Ni, Pd, Pt; Co, Rh, Ir; Fe, Ru, Os; Mn, Re; and Cr, Mo, W) interact with terrace sites of MgO. We found bonding with F_s and F_s^+ defects to be in general stronger than that with O^{2-} sites, except for Mn-, Re-, and Fe/F_s complexes. In M/F_s systems, electron density is accumulated on the metal center in a notable fashion. The binding energy on both kinds of O defects increases from 3d- to 4d- to 5d-atoms of a given group, at variance with the binding energy trend established earlier for the M/O^{2-} complexes, 4d < 3d < 5d. Regarding the evolution of the binding energy along a period, group 7 atoms are slightly destabilized compared to their group 6 congeners in both the F_s and F_s^+ complexes; for later transition elements, the binding energy increases gradually up to group 10 and finally decreases again in group 11, most strongly on the F_s site. This trend is governed by the negative charge on the adsorbed atoms. We discuss implications for an experimental detection of metal atoms on oxide supports based on computed core-level energies.

1. Introduction

For elucidating the chemical reactivity of supported metal systems, it is important to characterize at the microscopic level the technologically relevant interactions of d-metals with oxide ceramics.[1] Unfortunately, one succeeds only rarely in obtaining sufficiently detailed and comprehensive information on metal/oxide interfaces from experiments alone, because several factors which are difficult to control under experimental conditions act simultaneously. On the other hand, first-principles cluster and periodic slab-model calculations allow one to explore these factors separately and provide a complementary means for expanding our understanding of metal species supported on oxides.[2,3]

Metal atoms on oxides, as elementary building blocks of more extended supported metal systems, are of key importance for unraveling the initial stage of interface formation. Therefore, characterizing the bonding between metal atoms and oxide supports as well as the structure of such surface complexes is a prerequisite for describing larger supported moieties which result from metal nucleation and cluster growth. There is experimental evidence that metal nucleation often preferentially occurs at defects rather than at regular sites of well-ordered terraces of oxide surfaces;[4−6] among these sites, oxygen vacancies or color centers are considered to play a special role.[7] Nevertheless, structural and energetic parameters of the interaction of single d-metal atoms even with well-known surface point defects, such as neutral and charged oxygen vacancies (F_s left after removal of O atom and F_s^+ formed when O^- anion is missing) on the terraces of the ubiquitous oxide support MgO, have been theoretically quantified only for selected systems.[8−22]

† ICREA, Universitat de Barcelona, Parc Científic de Barcelona.
‡ Technische Universität München.
§ Russian Academy of Sciences.

(1) Bäumer, M.; Freund, H.-J. *Prog. Surf. Sci.* **1999**, *61*, 127.
(2) *Chemisorption and Reactivity on Supported Clusters and Thin Films*; Lambert, R. M., Pacchioni, G., Eds.; NATO ASI Series E, Vol. 331; Kluwer: Dordrecht, 1997.
(3) Rösch, N.; Nasluzov, V. A.; Neyman, K. M.; Pacchioni, G.; Vayssilov, G. N. In *Computational Material Science, Theoretical and Computational Chemistry*; Leszczynski, J., Ed.; Elsevier: Amsterdam, 2004; Vol. 15, p 365.
(4) Alstrup, I.; Møller, P. J. *Appl. Surf. Sci.* **1988**, *33−34*, 143.
(5) Meunier, M.; Henry, C. R. *Surf. Sci.* **1994**, *307−309*, 514.
(6) Haas, G.; Menck, A.; Brune, H.; Barth, J. V.; Venables, J. A.; Kern, K. *Phys. Rev. B* **2000**, *61*, 11105.
(7) Pacchioni, G. *ChemPhysChem* **2003**, *4*, 1041.
(8) Ferrari, A. M.; Pacchioni, G. *J. Phys. Chem.* **1996**, *100*, 9032.
(9) Matveev, A. V.; Neyman, K. M.; Yudanov, I. V.; Rösch N. *Surf. Sci.* **1999**, *426*, 123.
(10) Bogicevic, A.; Jennison, D. R. *Surf. Sci.* **1999**, *437*, L741.
(11) Ferrari, A. M.; Giordano, L.; Rösch, N.; Heiz, U.; Abbet, S.; Sanchez, A.; Pacchioni, G. *J. Phys. Chem. B* **2000**, *104*, 10612.
(12) Giordano, L.; Goniakowski, J.; Pacchioni, G. *Phys. Rev. B* **2001**, *64*, 75417.
(13) Abbet, S.; Riedo, E.; Brune, H.; Heiz, U.; Ferrari, A. M.; Giordano, L.; Pacchioni, G. *J. Am. Chem. Soc.* **2001**, *123*, 6172.
(14) Nasluzov, V. A.; Rivanenkov, V. V.; Gordienko, A. B.; Neyman, K. M.; Birkenheuer, U.; Rösch, N. *J. Chem. Phys.* **2001**, *115*, 8157.
(15) Bogicevic, A.; Jennison, D. R. *Surf. Sci.* **2002**, *515*, L481.
(16) López, N.; Paniagua, J. C.; Illas, F. *J. Chem. Phys.* **2002**, *117*, 9445.

10.1021/ja052437i CCC: $30.25 **© 2005 American Chemical Society**

Furthermore, most of these data calculated by density functional (DF) methods are not entirely consistent with each other or with results for regular MgO(001) surface sites for various methodological reasons. Some were obtained with cluster models, others with slab models; also, different exchange-correlation (xc) functionals have been employed, hampering a quantitative comparison. Thus far, DF results for the adsorption of the following d-metal atoms on F_s sites of MgO(001) have been communicated: Cu,[9,20,22] Ag,[8,9,15,19,20] Au,[15,17] Ni,[9,16] Pd,[8,9,11−15,18,19,21] Pt,[10,15] Rh,[15,19] Ir,[15] Ru,[15] and Nb.[15] Up to now, adsorption on *charged* F_s^+ centers has been challenging for periodic slab-model approaches. Thus, for the adsorption on this defect site, only cluster-model data are available and the list of atoms is even shorter: Cu,[9,22] Ag,[8,9,19] Ni,[9,16] Pd,[8,9,13,14,19,21] and Rh.[19] For some of the latter atoms, DF calculations were also performed on the doubly charged F_s^{2+} site (missing O^{2-} anion) of MgO(001).[8,14,16]

Recently we developed and implemented tools for embedding of cluster models in a so-called elastic polarizable environment (EPE),[14,23] which allows one to accurately describe the adsorption on oxide surfaces taking relaxation effects into account. Using this advanced computational technology, we studied the adsorption of single d-metal atoms on regular O^{2-} sites of MgO(001),[24] extending our earlier work[25] by three metal subgroups (Co, Fe, and Mn). The current study, carried out with exactly the same high-level computational approach as in ref 24, deals with interactions of 17 different single d-metal atoms with surface defects F_s and F_s^+ on MgO(001).

Thus, the present work reports a theoretical quantification of a major part of conceivable complexes which d-metal atoms formed on MgO(001) terraces. Together with the results on the M/O^{2-} systems,[24] this study provides a comprehensive database calculated at one and the same level, namely with one of the most accurate cluster-model approaches currently available. This database presents a unique opportunity to analyze and rationalize adsorption parameters of transition metal atoms on MgO(001) across the periodic table, which is one of the main goals of this study. In particular, we will demonstrate that (i) at variance with general belief, some d-metal atoms do form more strongly bound adsorption complexes at regular sites than at F-type surface defects; (ii) metal atoms in M/F_s complexes accumulate a considerable amount of electron density provided by the vacancy, and the trend of the adsorption energies is governed by this negative charge; and (iii) core-level energies of adsorbed metal atoms are characteristic and can be of help for detecting experimentally M/O^{2-}, M/F_s, and M/F_s^+ structures on MgO(001).

The paper is organized as follows. In section 2, we describe the cluster models employed to represent F_s and F_s^+ defects on MgO(001) terraces and we provide computational details. In section 3, we present the calculated structural and energetic parameters of adsorption complexes on the F_s and F_s^+ sites and we characterize their electron distribution. In section 4, we discuss peculiarities of and trends in the bonding of metal atoms on the oxygen vacancies compared to the regular sites. We also consider how the structure of adsorption complexes of transition metal atoms at oxides can be characterized with the help of calculated core-level energies. Conclusions are summarized in section 5.

2. Computational Details and Models

Spin-polarized calculations were performed using the linear combination of Gaussian-type orbitals fitting-function density functional (LCGTO-FF-DF) method[26] as implemented in the parallel computer code ParaGauss.[27,28] Two generalized-gradient approximation (GGA) xc functionals, BP86[29,30] and PBEN,[31] were used self-consistently. For the second- and third-row metal atoms, scalar-relativistic effects were taken into account employing a second-order Douglas−Kroll transformation to decouple electronic and positronic degrees of freedom of the Dirac−Kohn−Sham equation.[32,33]

We adopted the same flexible orbital basis sets as in our previous study:[24] (15s11p6d) → [6s5p3d] for 3d-atoms, (18s13p9d) → [7s6p4d] for 4d-atoms, (21s17p12d7f) → [9s8p6d4f] for 5d-atoms {for Au (21s17p11d7f) → [9s8p6d4f]}, (15s10p1d) → [6s5p1d] for Mg cations, and (13s8p1d) → [6s5p1d] for O anions. The latter basis set was also used to describe electrons trapped by the oxygen vacancies. All contractions specified in brackets (scalar-relativistic for 4d- and 5d-atoms) were of generalized, atomic form. Note that for 5d-atoms we used a more flexible scheme than in our earlier calculations,[9,25] with $m + 3$ contractions for each angular momentum where m is the number of occupied shells of a given atom. In the LCGTO-FF-DF method, an auxiliary basis set is employed to represent the electron charge density when evaluating the classical Coulomb (Hartree) part of the electron−electron interaction. For every atom, the auxiliary basis was constructed as follows: the exponents of s and r^2 fitting functions were generated from all or selected s and p orbital exponents, respectively, using a standard scaling procedure;[26] five p and five d "polarization" exponents have been added on each atomic center as geometric series with a factor 2.5, starting with 0.1 for p and 0.2 for d exponents.

The EPE cluster embedding has been described in detail elsewhere.[14] To be consistent with our model of the regular O^{2-} adsorption sites of the MgO(001) surface,[14,24] we employed here the clusters O_8Mg_9, neutral and positively charged, as a quantum mechanical (QM) part of the system to mimic the vacancies F_s and F_s^+, respectively. The coordination spheres of O anions at the cluster boundary were saturated by pseudopotential Mg^{2+} centers (Mg^{pp*}),[14,34] entirely without electrons; we employed 16 such centers in total. We used the same six-layer slab model of the MgO(001) surface, optimized previously[14,24] in an atomistic simulation at the classical molecular mechanical (MM) level,[35]

(17) Yang, Z. X.; Wu, R. Q.; Zhang, Q. M.; Goodman, D. W. *Phys. Rev. B* **2002**, *65*, 155407.
(18) Moseler, M.; Häkkinen, H.; Landman, U. *Phys. Rev. Lett.* **2002**, *89*, 176103.
(19) Giordano, L.; Del Vitto, A.; Pacchioni, G.; Ferrari, A. M. *Surf. Sci.* **2003**, *540*, 63.
(20) Zhukovskii, Yu. F.; Kotomin, E. A.; Borstel, G. *Vacuum* **2004**, *74*, 235.
(21) Giordano, L.; Di Valentin, C.; Goniakowski, J.; Pacchioni, G. *Phys. Rev. Lett.* **2004**, *92*, 096105.
(22) Del Vitto, A.; Sousa, C.; Illas, F.; Pacchioni, G. *J. Chem. Phys.* **2004**, *121*, 7457.
(23) Nasluzov, V. A.; Ivanova, E. A.; Shor, A. M.; Vayssilov, G. N.; Birkenheuer, U.; Rösch, N. *J. Phys. Chem. B* **2003**, *107*, 2228.
(24) Neyman, K. M.; Inntam, C.; Nasluzov, V. A.; Kosarev, R.; Rösch, N. *Appl. Phys. A* **2004**, *78*, 823.
(25) Yudanov, I.; Pacchioni, G.; Neyman, K.; Rösch, N. *J. Phys. Chem. B* **1997**, *101*, 2786.
(26) Dunlap, B.; Rösch, N. *Adv. Quantum Chem.* **1990**, *21*, 317.
(27) Belling, T.; Grauschopf, T.; Krüger, S.; Mayer, M.; Nörtemann, F.; Staufer, M.; Zenger, C.; Rösch, N. In *High Performance Scientific and Engineering Computing*; Bungartz, H.-J., Durst, F., Zenger, C., Eds.; Lecture Notes in Computational Science and Engineering, Vol. 8; Springer: Heidelberg, 1999; p 439.
(28) Rösch, N.; et al. *ParaGauss*, Version 3.0; Technische Universität München, 2004.
(29) Becke, A. D. *Phys. Rev. A* **1988**, *38*, 3098.
(30) Perdew, J. P. *Phys. Rev. B* **1986**, *33*, 8622; **1986**, *34*, 7406.
(31) Hammer, B.; Hansen, L. B.; Nørskov, J. K. *Phys. Rev. B* **1999**, *59*, 7413.
(32) Rösch, N.; Krüger, S.; Mayer, M.; Nasluzov, V. A. In *Recent Developments and Applications of Modern Density Functional Theory*; Seminario, J. M., Ed.; Elsevier: Amsterdam, 1996; p 497.
(33) Rösch, N.; Matveev, A.; Nasluzov, V. A.; Neyman, K. M.; Moskaleva, L.; Krüger, S. In *Relativistic Electronic Structure Theory—Applications*; Schwerdtfeger, P., Ed.; Elsevier: Amsterdam, 2004; Vol. 14, p 656.
(34) Fuentealba, P.; Szentpaly, L. V.; Preuss, M.; Stoll, M. *J. Phys. B* **1985**, *18*, 1287.

Table 1. Electron Configurations of d-Metal Atoms M, Used as Reference[a] for Binding Energies of Adsorption Complexes M/F_s and M/F_s^+ on MgO(001)

Cr d^5s^1	Mn d^5s^2	Fe d^6s^2	Co d^8s^1	Ni d^9s^1	Cu $d^{10}s^1$
Mo d^5s^1		Ru d^7s^1	Rh d^8s^1	Pd d^{10}	Ag $d^{10}s^1$
W d^5s^1	Re d^5s^2	Os d^6s^2	Ir d^7s^2	Pt d^9s^1	Au $d^{10}s^1$

[a] All states are of the highest possible spin. The configurations correspond to the lowest energies calculated at the all-electron BP86 level.

to generate the crystal environment of the resulting QM clusters. The environment affects the QM cluster both electrostatically, via the Madelung field, and mechanically, via short-range forces of the classical ions at the cluster boundary. Both the QM cluster and its MM environment, optimized to account for the vacancy formation, were allowed to relax in response to changes caused by the adsorbate so that the structure of the whole system was determined variationally by total energy minimization.[14] Except for the imposed C_{4v} point group symmetry, adsorption-induced relaxation was studied free of constraints with the BP86 functional.

Binding energies were computed with respect to the sum of the spin-polarized ground-state energy of a free metal atom and the energy of the relaxed MgO(001) model cluster.[24] These energies were counterpoise corrected[36] for the basis set superposition error in single-point fashion at the equilibrium geometry of the surface complexes. Spin contamination was quantified as the difference between the expectation value $\langle \hat{S}^2 \rangle$ of the total spin of the Kohn−Sham (KS) determinant and the ideal value, $S(S+1)$, where $S = n/2$ and n is the number of unpaired electrons. Most of the systems studied showed essentially no spin contamination, at most 1% with respect to $S(S+1)$; exceptions will be explicitly mentioned in the following. To characterize charge redistribution in the adsorption systems, we computed potential-derived charges (PDC)[37] which reproduce the electrostatic field in the area above the MgO(001) surface plane of the cluster models.

3. Results

Table 1 displays the lowest-energy electron configurations of free transition metal atoms calculated with the xc functionals BP86 and PBEN. For all atoms but Co and Ni, the KS ground-state configuration agrees with that detected experimentally.[38,39] The problem to define the proper reference energy of transition metal atoms in DF calculations has been thoroughly addressed elsewhere.[16,40,41] Therefore, this issue (pertinent here only to Co and Ni) will not be dealt with in the present work. The energies of the configurations from Table 1 (in the highest possible spin state) will be used in the following to determine adsorption energies of metal atoms on MgO, which will be corrected for the basis set superposition error with the help of the counterpoise method.

The calculated BP86 observables of the adsorption complexes M/F_s and M/F_s^+ studied are displayed in Tables 2 and 3, respectively. For those complexes which exhibit closely lying states, we show results for more than one electron configuration. We will now discuss these observables in more detail, starting with group 11 systems and moving to the left in the periodic system, to group 6.

Group 11: Cu, Ag, Au. The coinage metal atoms exhibit the simplest valence electron configuration, $d^{10}s^1$, among all atoms under scrutiny: a filled *n*d-shell and a singly occupied $(n+1)s$ orbital. This electron configuration is energetically well separated from the first excited configuration, d^9s^2, especially for Ag,[38,39] and thus very stable. At the F_s site of MgO(001), these atoms form a rather strong bond, with BP86 adsorption energies ranging from 180 to 310 kJ mol^{-1} (Table 2). Calculated large negative charges, −0.8 to −0.9 *e* on metal atoms, imply a considerable accumulation of electron density there, in line with the very low electronegativity of the F_s site on MgO(001),[9] which makes the two (almost free) electrons, accommodated by the vacancy, easily accessible for binding. Ag/F_s is the most weakly bound system. Relativistic effects notably facilitate d−s mixing for the Au atom of the Au/F_s complex and render it more strongly bound than Cu/F_s. The contribution of the adsorbate-induced relaxation to the adsorption interaction is very small, both energetically and structurally. This statement holds also for most of the adsorption complexes of other atoms under study; the few exceptions will be mentioned in due course. $M-F_s^+$ bonds of all three coinage metal atoms are stronger than the corresponding $M-F_s$ bonds, uniformly by ∼50 kJ mol^{-1} (cf. Tables 2 and 3). This is due to the coupling of the single valence s electron of the metal atoms with the single electron of the F_s^+ vacancy, leading to a rather strong covalent interaction. In turn, notably lowered charges on the metal of the M/F_s^+ systems imply a reduced contribution of the *polar* (electrostatic) bonding interaction.

Group 10: Ni, Pd, Pt. Experimentally, free Ni atoms feature almost degenerate low-energy triplet states corresponding to the configurations d^8s^2 and d^9s^1. The latter configuration is calculated to be 147 kJ mol^{-1} lower and is taken as reference in this study (see Table 1). For Pd and Pt atoms, the lowest energy terms of the electron configurations d^{10} and d^9s^1, respectively, are clearly favored over the lowest energy states of other electron configurations. Despite the open-shell nature of free Ni and Pt atoms, the ground states of the adsorption complexes of all three atoms of this group on F_s defects of MgO(001) are singlets. This finding is reminiscent of the configuration change from d^9s^1 to d^{10}, which occurs when Ni species interact with carbonyl ligands.[42,43] The group 10 atoms are considerably more strongly bound to the substrate, 278, 387, and 581 kJ mol^{-1} for Ni, Pd, and Pt, respectively (Table 2), than the coinage metal atoms. In fact, Pt at the F_s site is calculated to be most strongly bound among all atoms under study, both at F_s and F_s^+ MgO defects. This is also reflected by the adsorption height $Pt-Mg_4$ of Pt/F_s, which is drastically reduced, 30 pm, by relaxation from 176 to 146 pm. All three M/F_s species exhibit notably smaller negative metal charges (by absolute value) than their coinage metal analogues, but these charges nevertheless indicate a significant electron density transfer from the substrate. The particularly strong interaction $M-F_s$ at the neutral defect site can be traced back to the most favorable electron configuration $(a_1)^2(a_1^*)^0$ of these surface species,[9] where the bonding orbital

(35) Catlow, C. R. A.; Mackrodt, W. C. In *Computer Simulation of Solids*; Catlow, C. R. A., Mackrodt, W. C., Eds.; Lecture Notes in Physics, Vol. 166; Springer: Berlin, 1982; p 3.
(36) Boys, S. F.; Bernardi, F. *Mol. Phys.* **1970**, *19*, 553.
(37) Besler, B. H.; Merz, K. M.; Kollman, P. A. *J. Comput. Chem.* **1990**, *11*, 431.
(38) Moore, C. E. *Atomic Energy Levels*; U.S. Natl. Bur. Stand. Circ. No. 467; Government Printing Office: Washington, DC, 1952.
(39) Sansonetti, J. E.; Martin, W. C.; Young, S. L. *Handbook of Basic Atomic Spectroscopic Data*; National Institute of Standards and Technology: Gaithersburg, MD, 2004; online version 1.1 (http://physics.nist.gov/Handbook).
(40) Markovits, A.; Skalli, M. K.; Minot, C.; Pacchioni, G.; López, N.; Illas, F. *J. Chem. Phys.* **2001**, *115*, 8172.
(41) Markovits, A.; Paniagua, J. C.; López, N.; Minot, C.; Illas, F. *Phys. Rev. B* **2003**, *67*, 115417.
(42) Pacchioni, G.; Rösch, N. *Acc. Chem. Res.* **1995**, *28*, 390.
(43) Chung, S.-C.; Krüger, S.; Ruzankin, S. Ph.; Pacchioni, G.; Rösch, N. *Chem. Phys. Lett.* **1996**, *248*, 109.

Table 2. Calculated Parameters of Adsorption Complexes Formed by Single d-Metal Atoms M at Surface Oxygen Vacancies F_s of MgO(001)[a]

M	state[b]	z(M–Mg_4),[c] pm	Δr(Mg_4), pm	Δz(Mg_4), pm	q(M), e	$\Delta\epsilon$(M ns), eV	ΔE_b^{BP86}, kJ mol^{-1}	E_b^{BP86}, kJ mol^{-1}
Cu	$^2A_1$	173 (178)	3	0	−0.93	0.63	3	189
Ag	$^2A_1$	196 (193)	3	1	−0.81	0.42	3	178
Au	$^2A_1$	182 (184)	2	0	−0.85	0.48	5	311
Ni	$^1A_1$	137 (143)	4	2	−0.54	1.59	8	278
Pd	$^1A_1$	148 (157)	4	2	−0.60	0.58	14	387
Pt	$^1A_1$	146 (176)	4	4	−0.59	1.43	13	581
Co	$^2B_2$	169 (170)	2	1	−0.65	0.98	4	224
Rh	$^2B_2$	155 (160)	4	2	−0.53	1.03	4	342
Ir	$^2B_2$	152 (183)	5	5	−0.74	1.37	14	465
Fe	$^5A_2$	209 (218)	4	3	−0.37	1.01	7	127
	^3E	177 (193)	5	5	−0.39	1.74	8	123
Ru	$^5A_2$	216 (224)	4	2	−0.32	0.42	6	129
	$^3B_2$	172 (178)	6	6	−0.40	2.32	11	280
Os	$^5B_1$	196 (203)	5	3	−0.52	0.74	5	243
	$^3B_2$	163 (166)	5	6	−0.52	2.21	12	356
Mn	$^6A_1$	240 (242)	2	1	−0.30	1.04	3	74
	$^4B_1$	191 (218)	5	4	−0.38	2.42	15	57
Re	$^6B_1$	201 (204)	7	4	−0.30	1.27	10	85
	$^4B_1$	172 (175)	8	6	−0.30	2.24	15	143
Cr	$^7A_1$	224 (232)	3	0	−0.54	0.21	3	92
	$^5A_1$	218 (217)	5	3	−0.35	0.14	5	46
Mo	$^7A_1$	242 (245)	7	5	−0.60	0.59	9	109
	$^5A_1$	210 (210)	6	4	−0.24	1.04	22	114
W	$^7A_1$	217 (223)	6	3	−0.32	0.71	17	178
	$^5A_1$	207 (223)	5	2	−0.74	0.41	14	184

[a] z(M−Mg_4) is the height of M above the plane of the four nearest Mg atoms; Δr and Δz are the adsorption-induced displacements of the Mg_4 atoms in the radial direction and normal to the surface (a positive sign indicates an outward or upward shift, respectively); q(M) is the potential-derived charge of atom M; $\Delta\epsilon$(M ns) is the spin-averaged shift of the core M ns level with respect to the corresponding level of the adsorption complex M/O^{2-} (in the lowest-energy state listed in Table 4); E_b^{BP86} is the M−MgO binding (adsorption) energy; and ΔE_b^{BP86} is the energy gain due to the substrate relaxation caused by the presence of the adsorbate. [b] Assigned state based on the occupation numbers of the (high-spin) configuration from a spin-polarized calculation; assignments are unique in all cases considered. Systems with spin contamination >10%: Co/F_s, $^2B_2$, 66%; Fe/F_s, ^3E, 30%; Mn/F_s, $^4B_1$, 19%; Cr/F_s, $^5A_1$, 14%. [c] In parentheses, the height computed for the substrate fixed at the structure which was optimized without an adsorbate.

Table 3. Calculated Parameters of Adsorption Complexes Formed by Single d-Metal Atoms M at the Surface Oxygen Vacancy F_s^+ of MgO(001) (All Notations as in Table 2)

M	state	z(M–Mg_4), pm	Δr(Mg_4), pm	Δz(Mg_4), pm	q(M), e	$\Delta\epsilon$(M ns), eV	ΔE_b^{BP86}, kJ mol^{-1}	E_b^{BP86}, kJ mol^{-1}
Cu	$^1A_1$	160 (155)	1	3	−0.46	−1.97	6	242
Ag	$^1A_1$	186 (183)	2	5	−0.30	−2.25	8	229
Au	$^1A_1$	166 (165)	2	4	−0.42	−2.17	10	358
Ni	$^2A_1$	173 (168)	2	4	−0.21	−2.84	5	223
Pd	$^2A_1$	154 (155)	1	2	−0.30	−1.90	4	255
Pt	$^2B_2$	152 (154)	1	3	−0.19	−2.73	6	376
Co	$^3B_2$	183 (182)	2	4	−0.17	−2.18	5	202
Rh	$^3B_2$	179 (174)	0	2	−0.17	−2.02	3	238
Ir	^3E	165 (166)	2	4	−0.14	−2.55	6	297
Fe	$^4B_1$	190 (190)	2	4	−0.12	−1.19	8	166
	$^2B_2$	188 (188)	2	4	−0.13	−1.30	5	88
Ru	$^4B_1$	197 (198)	3	5	−0.07	−1.84	6	179
	$^2B_2$[a]	180 (177)	1	3	−0.14	−0.43	2	131
Os	$^4B_1$	175 (178)	4	6	−0.22	−1.62	6	274
	$^2A_1$	170 (172)	3	5	−0.24	−1.80	7	212
Mn	$^5B_1$[b]	197 (198)	2	4	−0.07	−0.39	5	81
Re	$^5B_1$	190 (191)	4	6	−0.01	−1.08	8	98
	$^3A_2$	201 (186)	2	4	−0.01	−1.54	5	44
Cr	$^6A_1$[c]	214 (212)	1	3	−0.02	−2.26	3	116
Mo	$^6A_1$[d]	222 (220)	1	3	0.06	−1.83	3	127
W	$^6A_1$	207 (208)	3	4	0.01	−1.83	5	192
	$^4A_2$	193 (193)	4	5	−0.01	−2.17	4	99

[a] Spin contamination 87%. [b] $^3A_2$ state calculated to be unbound (negative adsorption energy). [c] $^4A_2$ state calculated to be unbound (negative adsorption energy). [d] $^4A_2$ state calculated to be very weakly bound; E_b^{BP86} = 16 kJ mol^{-1}, z(M−Mg_4) = 207 pm.

a_1 (with a significant contribution of the vacancy) is filled whereas its antibonding counterpart a_1* is empty. This simple model predicts lower binding energies in the M/F_s^+ species where an electron is removed from the bonding orbital a_1. Our calculations indeed yield lower binding energies for the complexes on the F_s^+ site (Tables 2 and 3), by 55 kJ mol^{-1} for Ni and 132 kJ mol^{-1} for Pd. However, such a reduced covalent interaction appears to be not the only mechanism that leads to weaker bonding in the M/F_s^+ complexes of this group relative to the M/F_s species. In the Pt/F_s^+ system, the electron missing compared to the Pt/F_s complex is removed from the essentially nonbonding Pt 5d orbital b_2, the HOMO of Pt/F_s, instead of the

bonding orbital a_1, which is relatively stabilized in the case of Pt. Nevertheless, the $Pt-F_s^+$ bond is significantly weaker, by 205 kJ mol^{-1}, than the $Pt-F_s$ bond. Therefore, similarly to the coinage metal complexes, other effects are also important for binding, e.g., the electrostatic contribution associated with the transfer of electron density from the substrate to the adsorbate. The negative charges on the metal centers in M/F_s^+ are smaller by factors of 2 or more than in M/F_s but still remain noticeable, -0.2 to -0.3 *e*.

Group 9: Co, Rh, Ir. Our DF atomic reference for Co is the ground-state quartet d^8s^1 (Table 1), which at the BP86 level is 61 kJ mol^{-1} lower than the experimental quartet ground state d^7s^2.[38,39] The averaged experimental energy difference between the lowest terms of the configurations d^8s^1 and d^7s^2 is -40 kJ mol^{-1}.[39] In the adsorbed Co, Rh, and Ir moieties on F_s sites of MgO(001), partial spin quenching to doublet states (configurations b_2^1) is favored over the corresponding quartet states. Note, however, that the $^2B_2$ state of Co/F_s is severely spin contaminated, by 66% (Table 2); thus, a noncontaminated doublet state should be even more favored. The destabilization of the quartet states of the M/F_s species of this group relative to the doublets is at least in part due to the fact that the antibonding orbital a_1* is occupied in the quartets but remains empty in the doublets. The adsorption energies in these doublet-state complexes with respect to the corresponding DF atomic ground state are rather high: 224, 342, and 465 kJ mol^{-1} for Co, Rh, and Ir, respectively (Table 2). These values are only slightly smaller than those in the corresponding complexes of the Ni group. Negative charges accumulated in these moieties are even somewhat larger than in their group 10 analogues. The marked relaxation-induced reduction of the $Ir-Mg_4$ adsorption height is comparable to that mentioned above for the Pt/F_s complex. In all three M/F_s^+ complexes of group 9, triplet electron configurations are lowest in energy (Table 3): $(a_1)^1(b_2)^1$ (state $^3B_2$) for M = Co, Rh and $(e)^1(b_2)^1$ (state ^3E) for Ir, where a d orbital of e character is depleted, at variance with the mixed s−d orbital a_1 in the Co and Rh analogues. That a_1 level becomes significantly more stable in Ir/F_s, similar to what we have seen for Pt/F_s, relative to Ni/F_s and Pd/F_s. This is a consequence of relativistic stabilization of s orbitals. The M/F_s^+ species exhibit somewhat smaller binding energies, about 200−300 kJ mol^{-1}, than the corresponding M/F_s systems. Unlike for the latter complexes, the potential-derived charges on M were calculated to be only slightly negative, at most -0.2 *e*.

Group 8: Fe, Ru, Os. The high-spin metal atoms of this group as well as those in groups to their left in the periodic table often feature closely lying electron configurations; this statement also holds for the corresponding surface complexes. Therefore, from now on we will show, when applicable, results for the lowest states belonging to two multiplicities of each adsorption complex (Tables 2 and 3). The binding energies of the species Fe/F_s in the triplet and quintet states are very close in energy, whereas the $Fe-Mg_4$ heights differ by as much as ∼30 pm (Table 2). Note, however, the spin contamination of the calculated triplet. In the moieties Ru/F_s and Os/F_s, the triplet states are clearly preferred, in line with the reduced propensity of 4d- and 5d-atoms to form high-spin complexes. The three most stable systems M/F_s of the group 8 metals exhibit slightly weaker interactions with the substrate, 130−360 kJ mol^{-1}, than their *n*d analogues of group 9, and they show a somewhat smaller charge separation. In all complexes of Fe, Ru, and Os with the F_s^+ site, quartet states are definitely favored over the doublet states, by 50−80 kJ mol^{-1} (Table 3). The binding energies of the systems Fe/F_s^+, Ru/F_s^+, and Os/F_s^+ are slightly smaller than the values of their group 9 counterparts. The negative charge values on the adsorbates remain small.

The genealogy of the electron configurations (and states) characterizing the group 8 systems is rather complex. To illustrate this complexity, we start with the species Fe/F_s^+, Ru/F_s^+, and Os/F_s^+, the ground states of which all are $^4B_1$ quartets (Table 3), derived from the same electron configuration $(e)^2(b_2)^1$ (only open shells are shown). Addition of one electron to these complexes, formally transforming them into their M/F_s analogues, is accompanied by a distinct rearrangement of the electronic structure that depends on the metal. In Ru/F_s and Os/F_s, this extra electron and an electron depleted from the formerly closed shell $(a_1)^2$, mainly of metal d character, now both fill the orbital e, resulting in the triplet electron configuration $(a_1)^1(b_2)^1$, state $^3B_2$ (Table 2). In the 3d analogue Fe/F_s the enhanced propensity to form high-spin states is manifested in a decoupling of the $(b_1)^2$ shell and a concomitant promotion of the spin-flipped electron into the vacant orbital a_1*; see the discussion of group 10. Finally, for Fe/F_s one obtains the quintet state $^5A_2$ with configuration $(b_1)^1(a_1)^1(b_2)^1(a_1)^1$, energetically slightly favored over the lowest triplet state ^3E with configuration $(e)^3(b_2)^1$ (Table 2).

Group 7: Mn, Re. The two adsorption complexes M/F_s under discussion feature different spin states in their ground state (Table 2). Mn/F_s slightly prefers a sextet ground state over the quartet state which, however, is spin contaminated by 19%. On the other hand, for Re/F_s the quartet configuration is ∼60 kJ mol^{-1} lower in energy. These systems, Mn/F_s in particular, are among the most weakly bound M/F_s complexes studied here. The quartet and sextet configurations of the adsorption complex Mn/F_s, although energetically quite comparable, exhibit even more distinct adsorption heights (by 50 pm!) than the triplet and quintet configurations of Fe/F_s (see above). For both M/F_s^+ systems, we found the quintet state $^5B_1$ preferred. The Re complex at F_s^+ is notably less stable than its F_s analogue, whereas the Mn/F_s^+ species is almost as weakly bound as Mn/F_s. As a result, also among the M/F_s^+ complexes, the Mn and Re derivatives exhibit essentially the weakest adsorption bonds. The electronic structure of the complexes Mn/F_s^+ and Re/F_s^+ [configuration $(a_1)^1(e)^2(b_2)^1$ and a $^5B_1$ quintet state] correlates with that of their group 8 analogues which feature one valence electron more [configuration $(a_1)^2(e)^2(b_2)^1$ and a $^4B_1$ quartet state] (Table 3). Whereas the ground-state valence electron configuration of Re/F_s is the same as that of Os/F_s^+, $(e)^2(b_2)^1$, the configuration of the 3d-species Mn/F_s, $(b_1)^1(e)^2(b_2)^1(a_1)^1$, exhibits a higher spin state than Fe/F_s^+.

Group 6: Cr, Mo, W. This set of surface moieties M/F_s in very high spin states reveals probably the most complicated picture of structure and bonding. Indeed, only for the Cr/F_s system is the calculated energetics definite: a septet ground state is predicted (Table 2; the quintet $^5A_1$ features 14% spin contamination). We were not able to identify a clear energy preference for either the septet or the quintet states of Mo/F_s and W/F_s. However, no matter in which state these surface complexes of Cr and Mo are formed, their binding energies are expected to be the lowest among all the M/F_s adsorption systems

Table 4. Binding Energies (kJ mol^{-1}) Calculated with the GGA Functionals BP86 (E_b^{BP86}) and PBEN (E_b^{PBEN}) for the Most Stable State of Adsorption Complexes of Single d-Metal Atoms M at F_s and F_s^+ Defects of the MgO(001) Surface in Comparison with Complexes at Regular O^{2-} Sites

	M/F_s			M/F_s^+			M/O^{2-} [a]		
M	state	E_b^{BP86}	E_b^{PBEN}	state	E_b^{BP86}	E_b^{PBEN}	state	E_b^{BP86}	E_b^{PBEN}
Cu	$^2A_1$	189	167	$^1A_1$	242	218	$^2A_1$	93	72
Ag	$^2A_1$	178	152	$^1A_1$	229	203	$^2A_1$	46	25
Au	$^2A_1$	311	278	$^1A_1$	358	326	$^2A_1$	96	71
Ni	$^1A_1$	278	237	$^2A_1$	223	195	$^1A_1$	151	124
Pd	$^1A_1$	387	346	$^2A_1$	255	218	$^1A_1$	137	105
Pt	$^1A_1$	581	505	$^2B_2$	376	336	$^1A_1$	231	202
Co	$^2B_2$	224	194	$^3B_2$	202	181	$^2B_2$	118	87
Rh	$^2B_2$	342	298	$^3B_2$	238	207	$^2B_2$	125	93
Ir	$^2B_2$	465	390	^3E	297	259	$^2B_2$ [b]	136	112
Fe	$^5A_2$ [c]	127	110	$^4B_1$	166	125	$^5B_1$	136	112
Ru	$^3B_2$	280	257	$^4B_1$	179	154	$^5B_1$ [d]	86	60
Os	$^3B_2$	356	319	$^4B_1$	274	254	$^5B_1$	162	152
Mn	$^6A_1$ [e]	74	57	$^5B_1$	81	62	$^6A_1$	96	72
Re	$^4B_1$	143	110	$^5B_1$	98	71	$^6A_1$	146	125
Cr	$^7A_1$	92	79	$^6A_1$	116	106	$^7A_1$ [f]	61	51
Mo	$^5A_1$ [g]	114	88	$^6A_1$	127	111	$^5A_1$ [h]	56	30
W	$^5A_1$ [i]	184	151	$^6A_1$	192	166	$^5A_1$	151	121

[a] Reference 24. [b] $^4A_2$, $E_b^{BP86} = 134$ kJ mol^{-1}, ref 24. [c] ^3E, $E_b^{BP86} = 123$ kJ mol^{-1}, Table 2. [d] $^3B_1$, $E_b^{BP86} = 81$ kJ mol^{-1}, ref 24. [e] $^4B_1$, $E_b^{BP86} = 57$ kJ mol^{-1}, Table 2. [f] $^5A_1$, $E_b^{BP86} = 55$ kJ mol^{-1}, ref 24. [g] $^7A_1$, $E_b^{BP86} = 109$ kJ mol^{-1}, Table 2. [h] $^7A_1$, $E_b^{BP86} = 52$ kJ mol^{-1}, ref 24. [i] $^7A_1$, $E_b^{BP86} = 178$ kJ mol^{-1}, Table 2.

under scrutiny; only Mn/F_s is likely even more weakly bound. Also, a W adatom in either spin state exhibits the second-weakest binding to an F_s site among all other 5d-atoms under consideration (undercut only by Re). For the M/F_s^+ systems of group 6 atoms, the situation is somewhat simpler, at least as far as the most stable spin configuration is concerned, which is a sextet for all three moieties. These complexes, featuring essentially neutral metal adsorbates, were also calculated to be rather weakly bound.

4. Discussion

Table 4 and Figure 1 summarize calculated data to highlight and ascertain trends in the binding energy variation of *n*d-metal atoms in complexes with F_s and F_s^+ defects on the MgO(001) surface. These trends should also be compared with our findings for complexes of the same atoms on regular O^{2-} sites of MgO-(001).[24]

From Figure 1a (upper panel), one immediately recognizes that most M/F_s complexes are notably more strongly bound than their M/O^{2-} analogues (Figure 1a, bottom panel). This is in line with *all* previous calculations.[8−22] However, quite unexpectedly, there are some exceptions: Fe, Mn, and Re atoms are slightly more weakly bound (by ∼20 kJ mol^{-1} at most) at F_s defect sites than at regular O^{2-} sites. While all metal atoms exhibit negative charges, these three systems are also among those M/F_s complexes with the least charge separation (as measured by potential-derived charges; see Table 2, Figure 1b). A very substantial adsorption-induced increase of the electron density on the adsorbates (along with the subsequent increase of the electrostatic adsorbate−substrate attraction) appears to be an important stabilizing factor of M/F_s moieties. (Note that previously the charge separation analysis of selected M/F_s complexes[9] was based on the dynamic dipole moment, which indicated a considerably smaller substrate-to-adsorbate electron donation than the present PDC criterion.) M/F_s systems are furthermore stabilized compared to the corresponding M/O^{2-} analogues as Pauli repulsion with the substrate is reduced when the F_s vacancy is created because the electronic shells of the O center are no longer there. Finally, as outlined above for adsorbed metal atoms of group 10, covalent effects due to favorable filling of bonding/antibonding orbitals can be much more pronounced for complexes on oxygen vacancies than on regular sites of MgO(001). In fact, all these mechanisms work together and in general result in stronger M−F_s binding compared to that in M−O^{2-} complexes. This relative strengthening of the adsorption bond for the majority of the metal atoms under scrutiny exceeds 100 kJ mol^{-1} and reaches 350 kJ mol^{-1} for the most strongly bound Pt/F_s species (Table 4, Figure 1a). Concomitantly, metal−substrate distances (measured as the M−Mg_4 height, Table 2) are significantly shorter, by 50−60 pm, for some metals on the right-hand side of the periodic table than the previously computed values for the corresponding M/O^{2-} systems.[24]

In each of the examined groups of the periodic table, except for group 11, the 4d-atom is calculated to be adsorbed more strongly on the F_s site of MgO(001) than the 3d-atom, but more weakly than the 5d-atom: 3d < 4d < 5d. This is different from the binding energy trend within the group which we previously established for M/O^{2-} complexes (Figure 1a, bottom panel):[24] 4d < 3d < 5d. Regarding the energy variation of the M/F_s species along the period (Figure 1a, upper panel), atoms of group 7 are slightly destabilized with respect to their group 6 analogues. Moving to the right in each period, the binding energy increases gradually up to species of group 10 and finally it decreases again in group 11. This rather complicated trend reflects the complex character of the interactions experienced by d-metal atoms with defect sites of an oxide support, in particular with F_s sites of MgO(001). Note that these latter sites can be described to a good approximation by a very simple model[9] where only two electrons are treated quantum mechanically, moving in the field of the five immediate Mg^{2+} neighbors of the vacancy, represented by bare pseudopotential centers without a basis set, and a set of point charges representing the remaining substrate centers. For each metal, the strength of the resulting bond is determined by the delicate balance of the diverse contributions discussed in the preceding paragraph.

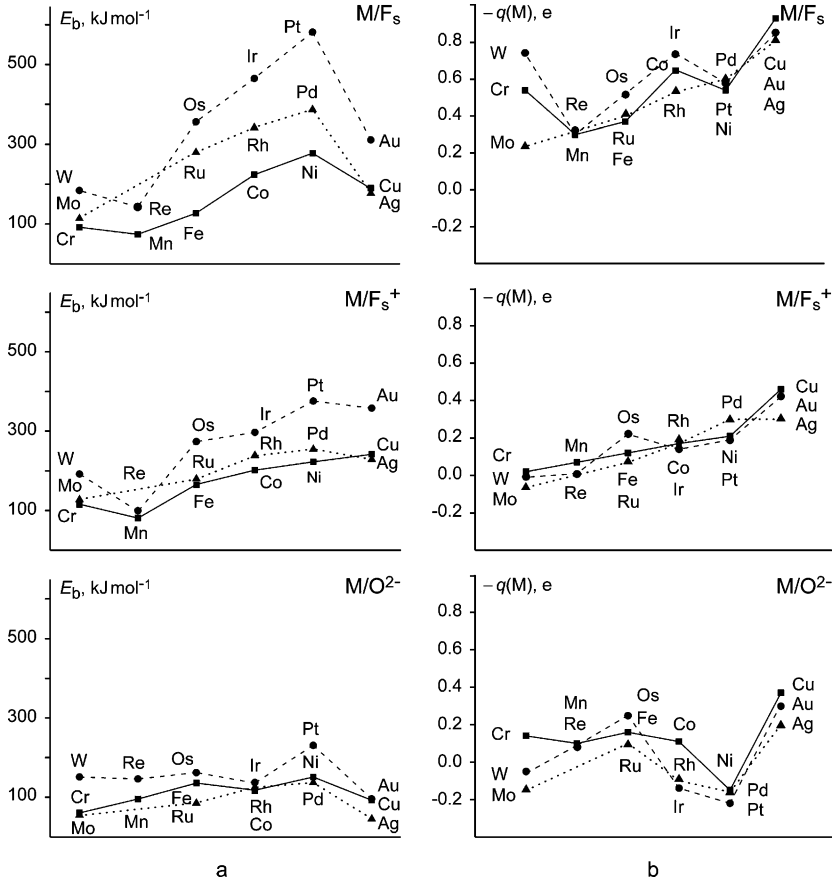

Figure 1. Trends in the BP86 binding energies (column a) and potential-derived charges (PDC) on adsorbates (column b) of the most stable adsorption complexes of single d-metal atoms on oxygen vacancies F_s (upper panels) and F_s^+ (middle panels) of MgO(001) surface in comparison with the energies and PDC values of the metal atoms on the regular O^{2-} sites (bottom panels of columns a and b, respectively; ref 24).

Nevertheless, there is an evident similarity in the general trend of the evolution of binding energies (Figure 1a, upper panel) and the alteration of PDC values (Figure 1b, upper panel) of the M/F_s complexes along the rows of the periodic table. Both the adsorption energies and the negative charges on the metal atoms exhibit an overall increase from the middle of each row to its right-hand side. There are some exceptions, in particular the complexes of the elements of group 6, which exhibit particularly high spin values, and the complexes of the elements of group 11; below, we will try to rationalize the values of the latter. This overall similarity implies that the accumulation of electron density on the adsorbates is a factor that governs the adsorption interactions of a series of *n*d-metal atoms with F_s vacancy sites on MgO(001) terraces. Interestingly, the trend in the PDC values is in fair agreement with the trend of the electronegativity values of the metal atoms.[44] However, only very crude adsorption energy estimates are possible on the basis of the electronegativity values; thus, high-level electronic structure calculations will continue to play a crucial role for quantifying this key characteristic.

In the literature, there are hardly reliable experimental data on the adsorption energetics of single d-metal atoms at F_s and F_s^+ sites of MgO(001). Moreover, precise benchmark calculations that treat electron correlation effects with sufficient accuracy in a realistic model do not seem practicable yet for the systems under discussion. On the other hand, one of the central problems of DF applications is the necessity to work with an approximate xc functional, as the exact functional is not known.[45] Without unambiguous reference data, one is unable to definitely establish which of the contemporary functionals provides the most accurate adsorption energies for elementary M/F_s complexes. However, one can very roughly estimate the general range of DF energies by comparing results obtained with several xc functionals. To this end, we compared binding energies for the M/F_s species from BP86 and PBEN calculations (Table 4).

Both sets of energies vary in very similar fashion with the adsorbed metal atoms. PBEN values are uniformly smaller by 10−20% than BP86 results; for the most strongly bound systems, this can amount to energy difference of up to 70−80 kJ mol^{-1}. Importantly, the trend of the uniformly reduced PBEN energies is apparently a systematic one, as it is also manifested for M/F_s^+ and M/O^{2-} complexes (Table 4). The hybrid B3LYP functional[46,47] yields binding energies for selected studied complexes M/F_s[19] that are 10−15% smaller than the corresponding PBEN values. The GGA functional PW91,[48] in combination with periodic slab models, provides energies for M/F_s species[15] that are in general close to our cluster-model BP86 data. As discussed presviously,[24] some larger deviations

(44) Huheey, J. E.; Keiter, E. A.; Keiter, R. L. *Inorganic Chemistry: Principles of Structure and Reactivity*, 4th ed.; HarperCollins: New York, 1993.

(45) Parr, R. G.; Yang, W. *Density Functional Theory for Atoms and Molecules*; Oxford University: Oxford, 1989.
(46) Becke, A. D. *J. Chem. Phys.* **1993**, *98*, 5648.
(47) Lee, C.; Yang, W.; Parr, R. G. *Phys. Rev. B* **1988**, *37*, 785.
(48) Perdew, J. P.; Chevary, J. A.; Vosko, S. H.; Jackson, K. A.; Pederson, M. R.; Singh, D. J.; Fiolhais, C. *Phys. Rev. B* **1992**, *46*, 6671.

are probably due to the neglect of spin-polarization effects.[15] For adsorption on metal surfaces,[31,49] the PBEN functional yields energies in close agreement with experiment, whereas the corresponding BP86 binding energies are somewhat larger in a systematic fashion. It remains to be seen whether these findings can be generalized to the energetics of supported metal particles on oxides.

The above considerations on the performance of various GGA and hybrid xc functionals are also valid for M/F_s^+ complexes. Thus, in the following we will discuss only observables calculated for the latter systems at the BP86 level (Tables 3 and 4, Figure 1).

The F_s^+ site of MgO(001), compared to the F_s site, exhibits two significant differences: (i) removal of an electron leaves one unpaired electron in the vacancy which is readily available for covalent bonding with an unpaired electron of a metal atom adsorbate, and (ii) concomitantly, the clear propensity of the F_s defects to donate electron density to the metal adsorbates (see above) is drastically reduced for the F_s^+ defects, as indicated, among others, by a strongly enhanced electron affinity of the latter.[9] The first factor is of particular importance for the M/F_s^+ complexes of Cu, Ag, and Au. These complexes feature the most favorable electron configuration $(a_1)^2(a_1^*)^0$ and binding energies which are at least 10% larger that those of their M/F_s analogues with the configuration $(a_1)^2(a_1^*)^1$. In contrast, the M/F_s^+ complexes formed by metal atoms of groups 9 and 10 are less stable than their M/F_s counterparts. Complexes of a given metal atom M of groups 6−8 at F_s and F_s^+ defects do not show a clear trend in their binding energies. Probably, the energy alterations of M/F_s^+ complexes of elements of groups 6−10, relative to their M/F_s congeners, are mainly determined by the combined effect of changes in the substrate−adsorbate charge transfer and the electron configuration (occupation of bonding/antibonding orbitals, high-/low-spin states). Except for Mn/F_s^+ and Re/F_s^+, all other M/F_s^+ complexes studied were calculated to be more strongly bound than the corresponding complexes M/O^{2-} at regular sites of MgO(001) (Table 4, Figure 1).

The overall trends in the adsorption energies of single d-metals on the F_s^+ sites of MgO(001) over a group of the periodic table are rather similar to those established above for the M/F_s systems. Indeed, in each group, the M/F_s^+ complex of the 5d-metal is most strongly bound, whereas that of the 3d-atom is least strongly bound, except for the Cu moiety which is $\sim$10 kJ mol^{-1} more stable than the Ag complex. Also, the evolution of the binding energies along a period shows a remarkable similarity for the M/F_s^+ and M/F_s complexes, which implies similarities in the electrostatic (polar) contribution to the bonding, caused by the charge separation between M and F_s^+ subsystems; cf. the trends of the binding energies and potential derived charges as depicted in the middle panels of Figure 1a,b. There are several noticeable differences between the trends of M/F_s and M/F_s^+ complexes: Energy variations within one period are smaller for M/F_s^+ systems, and the binding energy does not decrease at the end of the period, from Ni/F_s^+ to Cu/F_s^+. Also, the striking disparity of the binding energy and PDC trends when going from group 6 to group 7 complexes M/F_s, which feature a very high spin, is not seen for M/F_s^+ analogues.

Finally, we address opportunities for monitoring the interaction of atomically dispersed metal particles with regular and defect sites of metal oxide supports by means of X-ray photoelectron spectroscopy (XPS). Very recently, the shift of the Au 4f XPS peak from 85.8 eV at temperatures below 200 K to 85.4 eV at 300 K has been detected for atomic Au species deposited on $TiO_2(110)$[50] and attributed to the migration of some Au atoms from a variety of regular surface sites to oxygen vacancies that are a characteristic of the vacuum-annealed TiO_2-(110) surface.[51] Although, to the best of our knowledge, analogous experimental data are not yet available for metal atoms on MgO(001), it nevertheless seems worthwhile to study how core-level energies of metal atoms change with the sites of deposition on MgO(001) and whether similarities exist between adsorption complexes at oxygen vacancies of TiO_2-(110) and MgO(001).

As a first approximation, we focus on initial-state effects. For this purpose, we listed calculated spin-averaged shifts, $\Delta\epsilon$-(M *n*s), of Kohn−Sham core levels M *n*s for the complexes M/F_s (Table 2) and M/F_s^+ (Table 3) on MgO(001) relative to corresponding values of the M/O^{2-} adsorption complexes. Very interestingly, the shift $\Delta\epsilon$(Au 5s) = 0.48 eV for Au/F_s [along with $\Delta\epsilon$(Au 4f) = 0.44 eV, not shown in Table 2] is close to the value of 0.4 eV measured on $TiO_2(110)$.[50] The fact that core-level shifts of *all* metal atoms under study on F_s sites (including Au, Table 2) are positive, i.e., to lower binding energies, partly reflects the negative charge on the adsorbates. On the other hand, the adsorption complex Au/F_s^+ on MgO(001) features a very different shift $\Delta\epsilon$(Au 5s), −2.22 eV (Table 3). This allows one to exclude the analogue of this species on $TiO_2(110)$ from being a suitable candidate for rationalizing the experimental $\Delta\epsilon$(Au 4f) signature, all the more as all calculated values $\Delta\epsilon$(M *n*s) for M/F_s^+ complexes on MgO(001) are *negative* with respect to their reference M/O^{2-} (Table 3). The main negative contribution, −1.7 to −1.8 eV (as estimated by Kohn−Sham core-level shifts of a Mg cation used as internal reference in Au, Ag, and Cu complexes), is due to the overall elementary positive charge of the M/F_s^+ systems. Thus, core-level shifts of M/F_s and M/F_s^+ complexes relative to the corresponding energies of M/O^{2-} species appear to be characteristic for the type of oxygen vacancy that forms the adsorption site. In addition, calculated $\Delta\epsilon$ values are expected to help significantly in the structural assignment.

On the basis of calculated adsorption energies and core-level energies (Tables 2−4) for complexes of various metal atoms, one can predict results of experiments on MgO(001) terraces, which are similar to those reported in ref 50 for $Au/TiO_2(110)$. For instance, comparing the deposition of the coinage atoms Au, Ag, and Cu, one expects that diffusion of Ag to oxygen vacancy sites will take place at lower temperatures than for Cu and Au because Ag interacts more weakly on O^{2-} sites than Cu or Au. Also, the characteristic temperatures at which diffusion starts for Cu and Au should be rather similar. Assuming final-state effects (relaxation in the presence of a core-level hole at M) to be similar for M/O^{2-}, M/F_s^+, and M/F_s

(49) Yudanov, I. V.; Sahnoun, R.; Neyman, K. M.; Rösch, N. *J. Chem. Phys.* **2002**, *117*, 9887.
(50) Lee, S.; Fan, C.; Wu, T.; Anderson, S. L. *Surf. Sci.* **2005**, *578*, 5.
(51) Diebold, U. *Surf. Sci. Rep.* **2003**, *48*, 53.

complexes of the same metal, diffusion resulting in M/F_s species should be accompanied by a moderate positive M core-level shift of 0.4−0.6 eV. On the other hand, formation of M/F_s^+ moieties is expected to be manifested by a negative shift $\Delta\epsilon$ relative to M/O^{2-}. Many predictions like these, regarding the structure and properties of the complexes M/O^{2-}, M/F_s^+, and M/F_s, can be derived from the present calculated results, and these predictions will help in structural assignments of pertinent spectroscopic experiments that are expected to be carried out in the near future.

5. Conclusions

An accurate (scalar-relativistic) all-electron density functional method with a consistent cluster embedding in an elastic polarizable environment was used to study systematically metal atom adsorption on F_s and F_s^+ defects of the relaxed surface MgO(001) in comparison to the previously addressed adsorption on regular O^{2-} sites. Seventeen single d-metal adatoms of the third, fourth, and fifth rows of the periodic table were considered. The embedding method used treats both the central quantum mechanical region of the oxide clusters under study and their classical environment variationally, without artificial constraints for geometry optimization.

The adsorption energies presented, obtained with the BP86 and PBEN exchange-correlation functionals, corroborate the general picture of the interactions with oxygen vacancies on MgO terraces derived from studies of selected metal atoms. With few exceptions, these interactions with oxygen vacancies are significantly stronger than those with the regular sites and they are accompanied by a notable transfer of electron density from the F_s site to the d-metal adsorbate. In most groups, 4d-atoms are adsorbed more strongly than 3d-atoms, but more weakly than 5d-atoms, on both kinds of defects studied. This is at variance with the trend in binding energies within each group, 4d < 3d < 5d, which we previously established for M/O^{2-} complexes. As for the energy variation along the period, in both F_s and F_s^+ complexes, atoms of group 7 are slightly destabilized with respect to their group 6 analogues. Then, within a period, the binding energy increases gradually up to group 10 species and finally decreases again for group 11, most prominently on the F_s site. These trends appear to be governed by the negative charge on adsorbed atoms and their concomitant electrostatic interactions with the vacancy sites of MgO(001) terraces. The failure of DF methods to properly describe the ground-state electron configuration of Ni and Co atomic references may affect calculated values of the adsorption energy of these atoms.

Metal−substrate bonding in general is notably weaker in M/F_s^+ complexes than in their M/F_s analogues. We attribute this difference mainly to electrostatic stabilization of the latter species as a consequence of significant accumulation of electron density on the adsorbed atoms M, donated by the F_s vacancy. Covalent interactions may counteract this electrostatic stabilization and even alter the trend, making some M/F_s^+ complexes favored over their M/F_s congeners, as is the case for the Cu, Ag, and Au systems.

XPS core-level shifts of adsorbed metal atoms on MgO(001), approximated as differences of Kohn−Sham eigenvalues, revealed a characteristic dependence on the adsorption site. In combination with experimental XPS data, these calculated data open a way to distinguish between the M/F_s and M/F_s^+ structures on (001) terraces of MgO.

Although single adsorbed metal atoms represent *elementary* building blocks of more extended metal species supported on oxides, precise calculations on these systems and their rigorous analysis are complicated because usually several almost degenerate (magnetic) configurations are involved in the interaction with the substrate. One might invoke the constraint space orbital variation (CSOV)[52,53] method to separate and quantify various contributions to the adsorption energy. However, this approach does not appear promising for most of the systems under study due to their complex open-shell electronic structure.

An obvious extension of the present work will be a systematic study of interactions of single metal atoms with neutral and positively charged oxygen vacancies at lower coordinated surface sites of MgO, e.g. at steps, edges, and corners, where their formation is more justified thermodynamically.[54] Likely, these low-coordinated color centers are even stronger traps for single metal atoms than terrace vacancies.[55]

Acknowledgment. This work was supported by Deutsche Forschungsgemeinschaft, Volkswagen-Stiftung (follow-up grant I/73653), and Fonds der Chemischen Industrie.

Supporting Information Available: Complete ref 28. This material is available free of charge via the Internet at http://pubs.acs.org.

JA052437I

(52) Bagus, P. S.; Hermann, K.; Bauschlicher, C. W., Jr. *J. Chem. Phys.* **1984**, *80*, 4378.
(53) Neyman, K. M.; Ruzankin, S. Ph.; Rösch, N. *Chem. Phys. Lett.* **1995**, *246*, 546.
(54) Pacchioni, G.; Pescarmona, P. *Surf. Sci.* **1998**, *412/413*, 657.
(55) For instance, see ref 19 and references therein.